"Continuous cell injury promotes hepatic tumorigenesis in cdc42-deficient mouse liver"

van Hengel, Jolanda ; D'Hooge, Petra ; Hooghe, Bart ; Wu, Xunwei ; Libbrecht, Louis ; De Vos, Rita ; Quondamatteo, Fabio ; Klempt, Martina ; Brakebusch, Cord ; van Roy, Frans

Abstract

BACKGROUND & AIMS: The Rho small guanosine triphosphatase Cdc42 is critical for diverse cellular functions, including regulation of actin organization, cell polarity, intracellular membrane trafficking, transcription, cell-cycle progression, and cell transformation. This implies that Cdc42 might be required for liver function. METHODS: Mice in which Cdc42 was ablated in hepatocytes and bile duct cells were generated by Cre-loxP technology. Livers were examined by histologic, immunohistochemical, ultrastructural, and serum analysis to define the effect of loss of Cdc42 on liver structure. RESULTS: Mice lacking Cdc42 in their hepatocytes were born at Mendelian ratios. They did not show increased mortality but showed chronic jaundice. They developed hepatomegaly soon after birth, and signs of liver transformation, such as formation of nodules and tumors, became visible macroscopically at age 6 months. Hepatocellular carcinoma was observed 8 months after birth. Tumors grew slowly and lac...

Document type : *Article de périodique (Journal article)*

BASIC–LIVER, PANCREAS, AND BILIARY TRACT

Continuous Cell Injury Promotes Hepatic Tumorigenesis in Cdc42-Deficient Mouse Liver

JOLANDA VAN HENGEL,*,‡ PETRA D'HOOGE,* BART HOOGHE,§ XUNWEI WU,‖ LOUIS LIBBRECHT,¶ RITA DE VOS,¶ FABIO QUONDAMATTEO,# MARTINA KLEMPT,** CORD BRAKEBUSCH,‖ and FRANS VAN ROY*,‡

*Molecular Cell Biology Unit, and §Bioinformatics Core, Department for Molecular Biomedical Research, VIB, Ghent, Belgium; ‡Department of Molecular Biology, Ghent University, Ghent, Belgium; ‖Max Planck Institute for Biochemistry, Junior Group Regulation of Cytoskeletal Organization, Department of Molecular Medicine, Martinsried, Germany; ¶Department of Morphology and Molecular Pathology, University of Leuven, Leuven, Belgium; #Department of Histology, Georg August University Göttingen, Göttingen, Germany; and the **German Mouse Clinic and Institute of Molecular Animal Breeding, Ludwig Maximilian University, Munich, Germany

See editorial on page 875.

Background & Aims: **The Rho small guanosine triphosphatase Cdc42 is critical for diverse cellular functions, including regulation of actin organization, cell polarity, intracellular membrane trafficking, transcription, cell-cycle progression, and cell transformation. This implies that Cdc42 might be required for liver function.** ***Methods:*** **Mice in which Cdc42 was ablated in hepatocytes and bile duct cells were generated by Cre-*lox*P technology. Livers were examined by histologic, immunohistochemical, ultrastructural, and serum analysis to define the effect of loss of Cdc42 on liver structure.** ***Results:*** **Mice lacking Cdc42 in their hepatocytes were born at Mendelian ratios. They did not show increased mortality but showed chronic jaundice. They developed hepatomegaly soon after birth, and signs of liver transformation, such as formation of nodules and tumors, became visible macroscopically at age 6 months. Hepatocellular carcinoma was observed 8 months after birth. Tumors grew slowly and lacked expression of nuclear β-catenin. Lung metastases were observed at the late stage of carcinogenesis. Immunofluorescent examination and electron microscopy revealed severe defects in the liver. At the age of 2 months, the canaliculi between hepatocytes were greatly enlarged, although the tight junctions flanking the canaliculi appeared normal. Regular liver plates were absent. E-cadherin expression pattern and gap junction localization were distorted. Analysis of serum samples indicated cholestasis.** ***Conclusions:*** **We describe a mouse model in which chronic liver disease leads to hepatocarcinogenesis.**

The Ras superfamily of guanosine triphosphate (GTP)-binding proteins relays extracellular ligand–mediated signals to cytoplasmic signaling pathways. Cdc42 is a ubiquitously expressed member of Rho-GTPases, a subfamily of small GTPases. In general, Rho-GTPases function as molecular switches because they flip back and forth between an inactive GDP-bound form and an active GTP-bound state. The activated GTP-bound Rho-GTPases interact with a broad spectrum of effector molecules, such as N-WASP, PAK1-4, and partitioning-defective-6 (Par6), which in turn regulate the actin cytoskeleton, microtubule network, cell polarity, proliferation, apoptosis, endocytosis, and secretion.

The liver is endowed with many specialized functions, most of which are controlled by hepatocytes. Establishment of cell junctions between these parenchymal cells is indispensable for their functions. In this respect, most attention has focused on the adherens and gap junctions. Several hepatocyte-specific functions, including albumin secretion, ammonia detoxification, glycogenolysis, and bile secretion, require the presence of these junctions (reviewed by Vinken et al[1]). However, most of the results have been obtained from in vitro studies.

Adherens junctions in hepatocytes consist of the transmembrane molecules E-cadherin or N-cadherin linked to the actin cytoskeleton by a number of catenins. Gap junctions in hepatocytes are composed of connexin (Cx)32 and Cx26. Expression of Cx32 is restricted mainly to hepatocytes, and numerous articles have reported se-

Abbreviations used in this paper: aPKC, atypical protein kinase C; BrdU, bromodeoxyuridine; Cdc42HeKO mice, mice with Cdc42fl/fl; AlbCre, AlbCre genotype; CK, cytokeratin; Cx, connexin; GTP, guanosine triphosphate; Par, partitioning-defective.

0016-5085/08/$34.00
doi:10.1053/j.gastro.2008.01.002

rious liver dysfunction in Cx32-Knock-out (KO) mice.[2] Two cell-polarity protein complexes, which are highly conserved throughout evolution, localize at tight junctions in vertebrate epithelia (reviewed by Margolis and Borg[3]). One complex is Par-3/Par-6/atypical protein kinase C (aPKC). The 2 complexes participate in the establishment of apical-junctional complexes and apicobasal cell polarity. Rho-GTPases play important roles in controlling the apical complex. Cdc42 binds to Par-6 and increases the activity of aPKC within the Par-3/Par-6/aPKC complex.[4]

Mice totally deficient in Cdc42 function die during embryonic development.[5] Recently, Cdc42 was deleted in the epidermis[6] and in the developing mouse brain.[7,8] Because the liver is composed of plates of highly polarized hepatocytes, Cdc42 could play an important role in liver morphogenesis and homeostasis. We addressed this by ablating Cdc42 specifically in a portion of hepatoblasts and hepatocytes.

Several lines of evidence implicate Rho family members in a variety of important processes in cancer, including cell survival, proliferation, invasion, metastasis, and angiogenesis.[9] Recent observation of abnormal *Cdc42* copy numbers in neuroblastomas led Valentijn et al[10] to propose Cdc42 as a candidate tumor-suppressor gene in these tumors. Loss of heterozygosity for a chromosomal region that includes the *Cdc42* gene was described in cholangiocarcinoma patients,[11] which is in line with a possible tumor-suppressor role for Cdc42. In the present study, we show that Cdc42 modulates cell polarity and cell-cycle control in hepatocytes in vivo. Moreover, mice lacking Cdc42 expression in hepatocytes develop hepatocellular carcinomas (HCCs).

Materials and Methods

Generation of Cdc42fl/fl;Alb Cre Mice

Transgenic Cdc42 flox/flox mice[12] were crossed with mice expressing Cre recombinase under control of a rat albumin promoter.[13] All the mice analyzed had a genetically mixed background of C57BL6, 129, and Swiss strains. Mice were kept in standard housing according to the Belgian rules on animal welfare. β-galactosidase staining was performed according to standard procedures on the offspring of a cross between Cdc42-Alb Cre mice and the ROSA26 strain.

Immunofluorescent Analysis

Livers were frozen in cryo-embedding compound (Microm International, Walldorf, Germany) and sectioned at 6 μm using a cryostat. Sections were air-dried and fixed in freshly prepared 4% paraformaldehyde. Cells were permeabilized with 0.2% Triton X-100 in phosphate-buffered saline (PBS) for 5 minutes, washed twice in PBS, and treated with blocking buffer for 20 minutes. Thereafter, sections were incubated with primary antibody for 2 hours at room temperature or overnight at 4°C, washed again, and incubated with an Alexa-coupled anti-rabbit secondary antibody (Molecular Probes, Eugene, OR) for 60 minutes. Sections were embedded in Vectashield with DAPI (Vector, Burlingame, CA) and examined with an Axiophot microscope (Zeiss, Jena, Germany) or confocal laser scanning microscope (Leica, Mannheim, Germany).

Ultrastructural Analysis

For electron microscopy, small pieces of liver were immediately fixed overnight in 2.5% glutaraldehyde, 0.1 mol/L phosphate buffer at 4°C. After 1 hour postfixation in 1% osmium tetroxide in 0.1 mol/L phosphate buffer at 4°C, the samples were dehydrated and embedded in epoxy resin. Ultrathin sections of 60 nm were cut, stained with uranyl acetate and lead citrate, and examined at 50 kV using an EM 900 electron microscope (Zeiss). Images were recorded digitally with a ProgRes C14 camera system (Jenoptik, Jena, Germany) operated with Image-Pro express software (Media Cybernetics, Silver Spring, MD).

Biochemical Analysis

Serum samples of knockout and age-matched control mice (5 weeks to 3 months of age) were analyzed as detailed in Materials and Methods in supplementary data (see supplementary material online at www.gastrojournal.org).

Results

Generation of Mice Lacking Cdc42 in Hepatocytes

To study how Cdc42 contributes to morphogenesis and cell-junction formation in polarized epithelia, we inactivated Cdc42 in mouse hepatocytes. Mice carrying 2 floxed Cdc42 alleles were crossed with mice carrying a single floxed Cdc42 allele in addition to the Cre-recombinase gene under control of the rat albumin promoter.[13] Progenies were born at the expected Mendelian ratio and survived for up to 2 years. Hepatocyte-specific Cdc42 knockout mice (with the Cdc42fl/fl;AlbCre genotype [Cdc42HeKO]) showed growth retardation, hypertrophy of the liver, and chronic jaundice. The liver weight to body weight ratio of Cdc42HeKO mice was 2-fold higher than that of control littermates at 2 and 4 months of age (Figure 1*A*). From 6 months of age, first small and later large nodules were visible macroscopically on the liver (Figure 1*B*).

Western blot analysis showed that Cdc42 was depleted almost completely in the livers of 5- and 10-week-old Cdc42HeKO mice, in contrast to the Cdc42fl/+;AlbCre and Cdc42fl/fl controls (Figure 1*C*). The small amount of residual Cdc42 probably was expressed by endothelial, stellate, and inflammatory cells. To examine the efficiency of recombination as a function of age, Southern blot

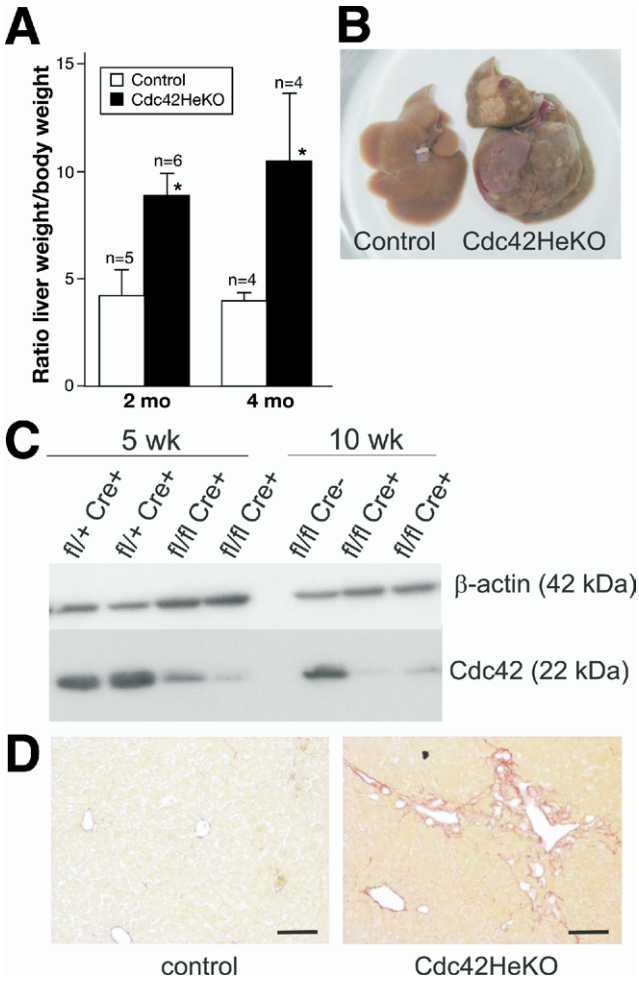

Figure 1. Initial analysis of Cdc42HeKO mice with Cdc42 ablation in hepatocytes and cholangiocytes. (*A*) The liver weight/body weight ratio was determined 2 and 4 months after birth. Results are expressed as the mean ± SD. The number of mice per group is indicated. Statistical differences were determined by Wilcoxon rank sum test: $^*P < .05$. □, Control; ■, Cdc42HeKO. (*B*) Compared with the control liver, the liver from a Cdc42HeKO mouse is enlarged and has many nodules of different sizes on its surface (both mice were 10 months old). (*C*) Western blot of proteins isolated from mice aged 5 and 10 weeks. Cdc42 is diminished considerably in Cdc42HeKO livers (fl/fl Cre+ mice), compared with control livers (fl/+ Cre+ mice). β-actin was used as a loading control. (*D*) Sirius red staining of the livers of Cdc42HeKO mice shows accumulation of collagen around the portal region. Magnification bars, 200 μm.

analysis was performed on liver genomic DNA isolated from control and Cdc42HeKO mice. The efficiency of recombination was only about 50% at 3 days, but later increased to more than 80% (shown for 3.5 and 11 months in supplementary Figure 1*A* and *B*; see supplementary material online at www.gastrojournal.org). Crossing the mutant mice with mice expressing the *lacZ* gene in a Cre-dependent way confirmed that most hepatocytes had recombined loxP sites at the age of 4 months. Distribution of Cre activity was somewhat heterogeneous in Cdc42HeKO-Rosa26 livers compared with the positive control AlbCre-Rosa26 livers (supplementary Figure 2*A*; see supplementary material online at www.gastrojournal.org). Macroscopically visible tumors were isolated and their DNA was examined for the presence of different modified alleles (supplementary Figure 1*B*; see supplementary material online at www.gastrojournal.org). The nodules consisted of a large fraction of cells with recombined loxP sites, and therefore lacking expression of Cdc42 protein (supplementary Figure 1*C*; see supplementary material online at www.gastrojournal.org).

Cdc42 Mutant Mice Develop Jaundice

Analysis of sera from control and Cdc42-deficient mice (Table 1) revealed significant differences in alanine aminotransferase (ALT), aspartate aminotransferase (AST), and alkaline phosphatase levels, indicative of damaged hepatocytes in the mutant mice. Total cholesterol and triglyceride levels in sera were not significantly different in the 2 strains. Total and conjugated bilirubin were significantly higher in Cdc42HeKO mice than in controls. The accumulation of conjugated bilirubin in Cdc42HeKO mice implies a posthepatocytic defect, such as impaired bile transport. Figure 1*D* shows liver sections stained with Sirius red. No fibrosis is observed in control livers (left panel). In contrast, fibrosis was evident in livers of 2-week-old Cdc42HeKO mice (not shown), and increased in severity at 2 and 4 months (right panel). We never observed cirrhosis in Cdc42HeKO livers.

HCC Formation in Cdc42 Mutant Livers

Histologic analysis of liver specimens from 2-month-old Cdc42HeKO mice revealed no major abnormalities in lobular architecture. Hepatic plates in Cdc42HeKO mice were more irregular than in control littermates (Figure 2*A*). Most obvious in the mutant livers by the age of 2 months were enlarged bile canaliculi, vacuoles, large-cell dysplasia, and cell damage apparent from ballooning and clumping of cytoplasm (Figure 2*A*, insets). At 2 months of age no tumors were visible macroscopically, whereas at 6 months tiny nodules were

Table 1. Liver-Specific Serum Markers in Control and Cdc42HeKO Mice

Serum marker	Control mice	Cdc42HeKO mice
Total cholesterol measurement, *mmol/L*	103 (7.1)	87 (21.3)
Alanine aminotransferase level, *U/L*	19 (6.2)	175 (92.5)
Aspartate aminotransferase level, *U/L*	34 (9.8)	152 (75.8)
Alkaline phosphatase level, *U/L*	96 (33.4)	507 (123.2)
Triglyceride level, *mg/dL*	96 (4.7)	85 (23.8)
Conjugated bilirubin level, *mg/dL*	0 (0)	3.05 (1.35)
Total bilirubin level, *mg/dL*	0 (0.08)	5.81 (3.41)

NOTE. Means and SDs shown of 8 Cdc42HeKO mice and 8 controls, 5 weeks to 3 months after birth.

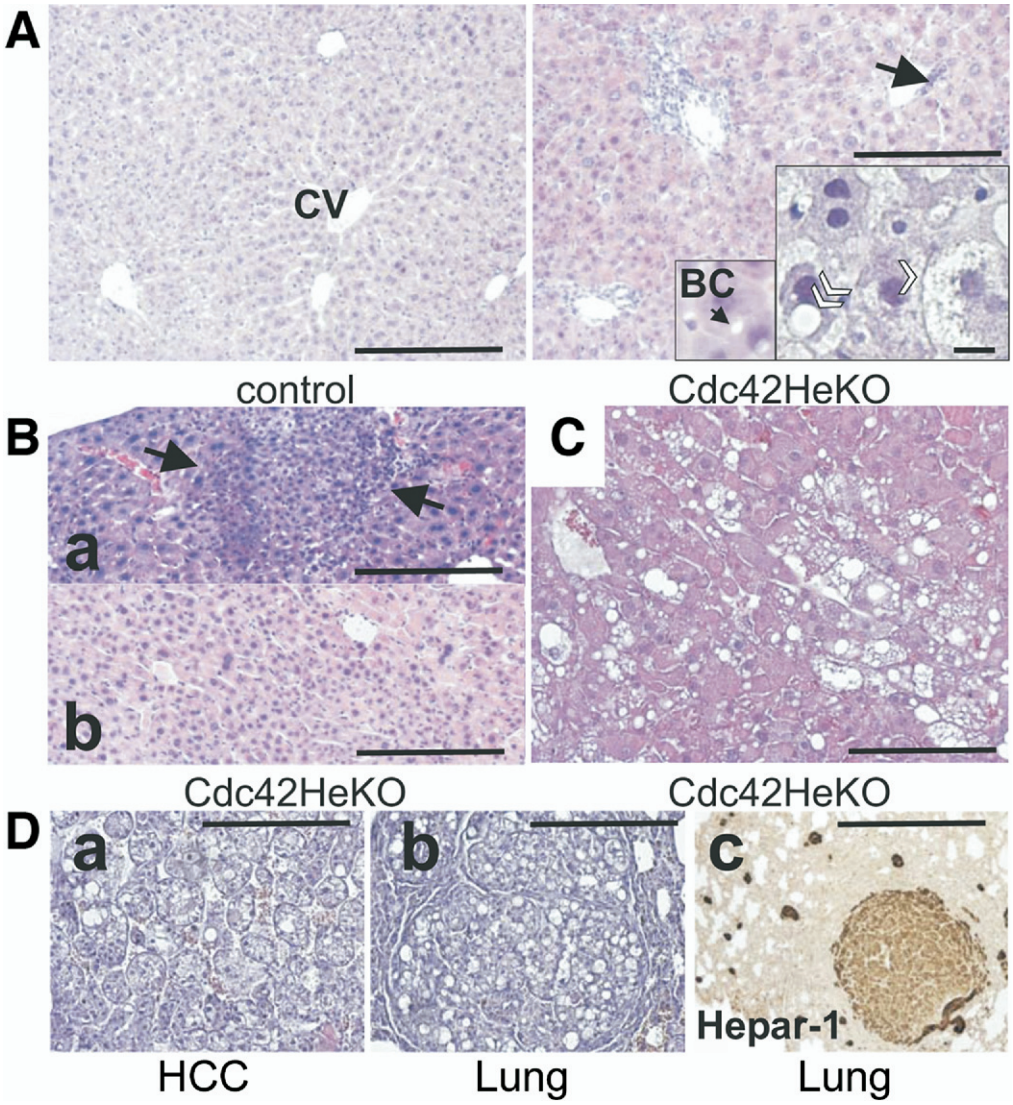

Figure 2. Alterations in liver histology caused by Cdc42 deletion. (*A*) Liver sections of 2-month-old mice were stained with H&E. Cdc42-deficient hepatocytes were histologically heterogeneous. The arrow indicates a focus of large-cell dysplasia consisting of hepatocytes showing nuclear and cellular enlargement. The smaller inset shows enlarged bile canaliculi (arrow). In the second inset the damage to hepatocytes is apparent from ballooning of the cells and clumping of the cytoplasm (white arrowhead). Hepatocyte vacuolization is visible (double white arrowhead). (*B*) Small-cell dysplasia (a, between arrows) and oncocytic foci without pushing margins (b) were visible in Cdc42-deficient livers starting at age 6 months. (*C*) Microscopic examination of a 15-mm nodule revealed that it consisted of hepatocytes organized in greatly widened trabecules forming a well-differentiated HCC. The hepatocytes showed moderate nuclear atypia, and the vacuoles pointed to steatosis. (*D*) In 18-month-old Cdc42HeKO mice, HCC (a) leads to lung metastases (b) as proven by Hepar-1 staining (c). Most magnification bars, 400 μm; except insets in *A*, 20 μm; and Hepar staining in *D*, 1 mm.

observed in each liver. Small-cell dysplasia and oncocytic foci were visible at that time (Figure 2*B*). At 8 months macroscopically visible nodules of different sizes were present in all Cdc42HeKO mice examined. These nodules showed typical HCC histology (exemplified in Figure 2*C*). As mentioned earlier, both Southern and Western analyses showed that these nodules were derived from cells in which the Cdc42 locus was targeted (supplementary Figure 1*B* and *C*; see supplementary material online at www.gastrojournal.org). Finally, we observed different lung metastases in some 18-month-old Cdc42HeKO mice (Figure 2*D*). Expression of the hepatocellular differentiation marker Hepar was assessed to prove the hepatic origin of the metastases. Based on cytokeratin-19 (CK19) and histologic stainings, we observed no cholangiocarcinoma in Cdc42HeKO mice.

Despite formation of tumors in Cdc42HeKO mice, their lifespan was unchanged. We followed up 35 Cdc42HeKO mice, of which 2 died by the age of 8 months, and 27 control mice, of which 1 died within the same period. All 16 analyzed Cdc42HeKO mice developed HCC after 7–9 months, but no control mice developed HCC. After HCC development (7–9 mo) we followed up 16 KO and 14 control mice. Of these, 1 KO mouse died at 11 months but no control mice died during the observation period. From this group we kept 6 KO mice and 2 control mice to the age of 18 months; all of them survived. HCC grew very slowly, which could account for the normal lifespan of the KO mice. Had they grown fast, the mass of the liver could have compressed neighboring organs, and metastasis to the lungs could have compromised respiration. The only lung metastases we observed were in 2 of the six 18-month-old Cdc42HeKO mice (see also earlier). The number of mice we analyzed was too small to determine if one of the sexes is more susceptible to HCC formation.

Mechanisms of Weight Increase of Cdc42 Mutant Livers

The number of hepatocytes bearing mitotic figures was increased at all stages in Cdc42HeKO livers

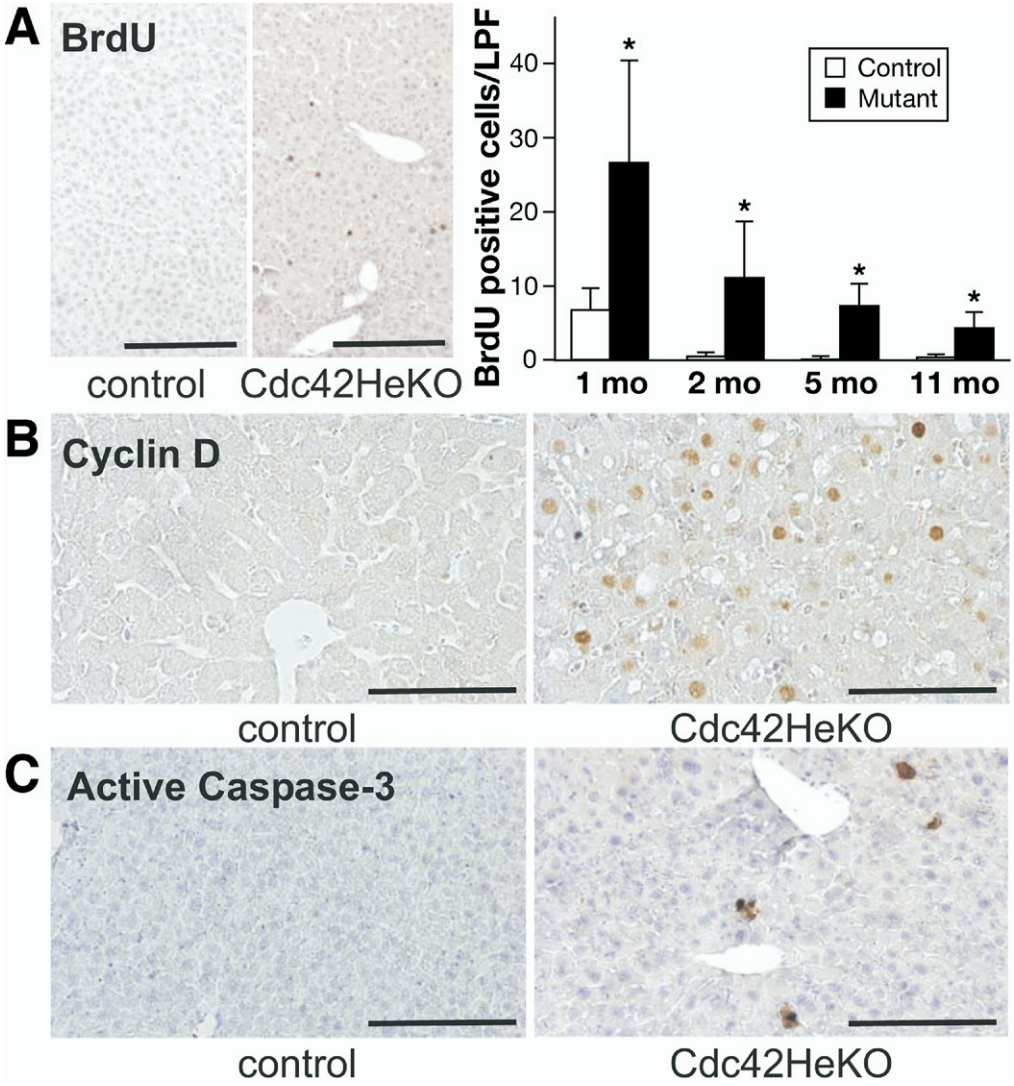

Figure 3. Increased proliferation and apoptosis in Cdc42HeKO livers. (*A*) Identification of proliferating hepatocytes by BrdU labeling. Liver sections of age-matched control and Cdc42HeKO mice were compared. The bar graph on the right shows the number of BrdU-positive cells per low-power field (LPF, 10× ≈ 629,748 μm^2), averaged on 2 livers and 10 images per mouse. Labeling was performed 1, 2, 5, and 11 months after birth. Statistical differences were determined using the Wilcoxon rank sum test: *$P < .05$. □, Control; ■, mutant. (*B*) Hepatocytes in 2-month-old control mice expressed no cyclin D1, whereas dysplastic hepatocytes in Cdc42HeKO livers were strongly positive for cyclin D1. (*C*) Hepatocytes of 2-month-old control mice did not stain for active caspase-3, whereas several Cdc42HeKO hepatocytes expressed active caspase 3. Magnification bars, 400 μm.

(data not shown). Therefore, the number of S-phase hepatocytes was determined by measuring bromodeoxyuridine (BrdU) incorporation in livers of mutant and control mice at various ages. For each age, the BrdU incorporation rate was significantly much higher in Cdc42HeKO livers than in controls, but there was no particular cellular distribution pattern (Figure 3*A*). Cyclin D1/2 also was induced strongly in mutant hepatocytes (Figure 3*B*). This might have been the result of accumulation of stabilized β-catenin protein in the nuclei and the resulting activation of the Wnt signaling pathway. However, in Cdc42HeKO livers and tumors we did not observe nuclear β-catenin, truncated β-catenin protein, aberrant β-catenin messenger RNA (mRNA), or mutations in the β-catenin gene (supplementary Figure 3; see supplementary material online at www.gastrojournal.org). Another argument in favor of β-catenin–independent regulation is the expression of glutamine synthetase. We observed no activation of this enzyme in Cdc42HeKO mouse livers, neither in young mice nor in tumors from old mice (supplementary Figure 3*D*; see supplementary material online at www.gastrojournal.org).

Increased death of hepatocytes in Cdc42HeKO mice was indicated by the high activities of ALT and AST (Table 1), and by histologic evidence for the presence of apoptotic and ballooning hepatocytes. Staining for active caspase-3 confirmed the existence of apoptotic hepatocytes in Cdc42HeKO mice compared with controls (Figure 3*C*). Thus, the absence of Cdc42 in hepatocytes leads to both cell damage and increased cell proliferation. Because the latter was only partly counterbalanced by compensatory apoptosis, livers became hyperplastic and tumors formed. Another reason for the increased liver weight is the larger size of Cdc42HeKO hepatocytes. This was determined by counting hepatocytes in 10 nonoverlapping high-power fields (supplementary Figure 4*A*; see supplementary material online at www.gastrojournal.org). Cdc42HeKO livers contain fewer hepatocytes per unit area because Cdc42-deficient hepatocytes generally are larger than control hepatocytes. One more reason for

the increased liver weight in Cdc42HeKO mice is biliary proliferation (supplementary Figure 4*B*; see supplementary material online at www.gastrojournal.org). Finally, the deposit of extracellular matrix material, revealed by Sirius red staining (Figure 1*D*), also contributed to the increase in liver weight.

Ultrastructural Analysis of Cdc42-Deficient Hepatocytes and Cholangiocytes

We compared the ultrastructure of hepatocytes in control mice and Cdc42HeKO mice at 2 months of age by electron microscopy. In control mice the bile canaliculi of hepatocytes had many largely regular slender microvilli. The lateral cell membranes contained junctional complexes, tight and intermediate junctions, and desmosomes, which seal the canalicular lumen and maintain the canalicular-sinusoidal barrier (Figure 4*A* and *C*). In the Cdc42HeKO mice, however, severe changes in the bile canaliculi were evidenced by varying degrees of dilation, invagination, and varicosity. These changes were associated with morphologic irregularities and decreased numbers of microvilli, which occasionally formed microvillous blebs (Figure 4*B*). The marginal microvilli, those closest to the tight junctions, and the junctions themselves were preserved even when canalicular dilation was severe (Figure 4*D*).

The pericanalicular ectoplasm containing actin filaments often appeared thickened in mutant hepatocytes; a prominent sheath of intermediate cytokeratin filaments surrounding the ectoplasmic rim was often observed. At the sinusoidal pole the irregular microvilli

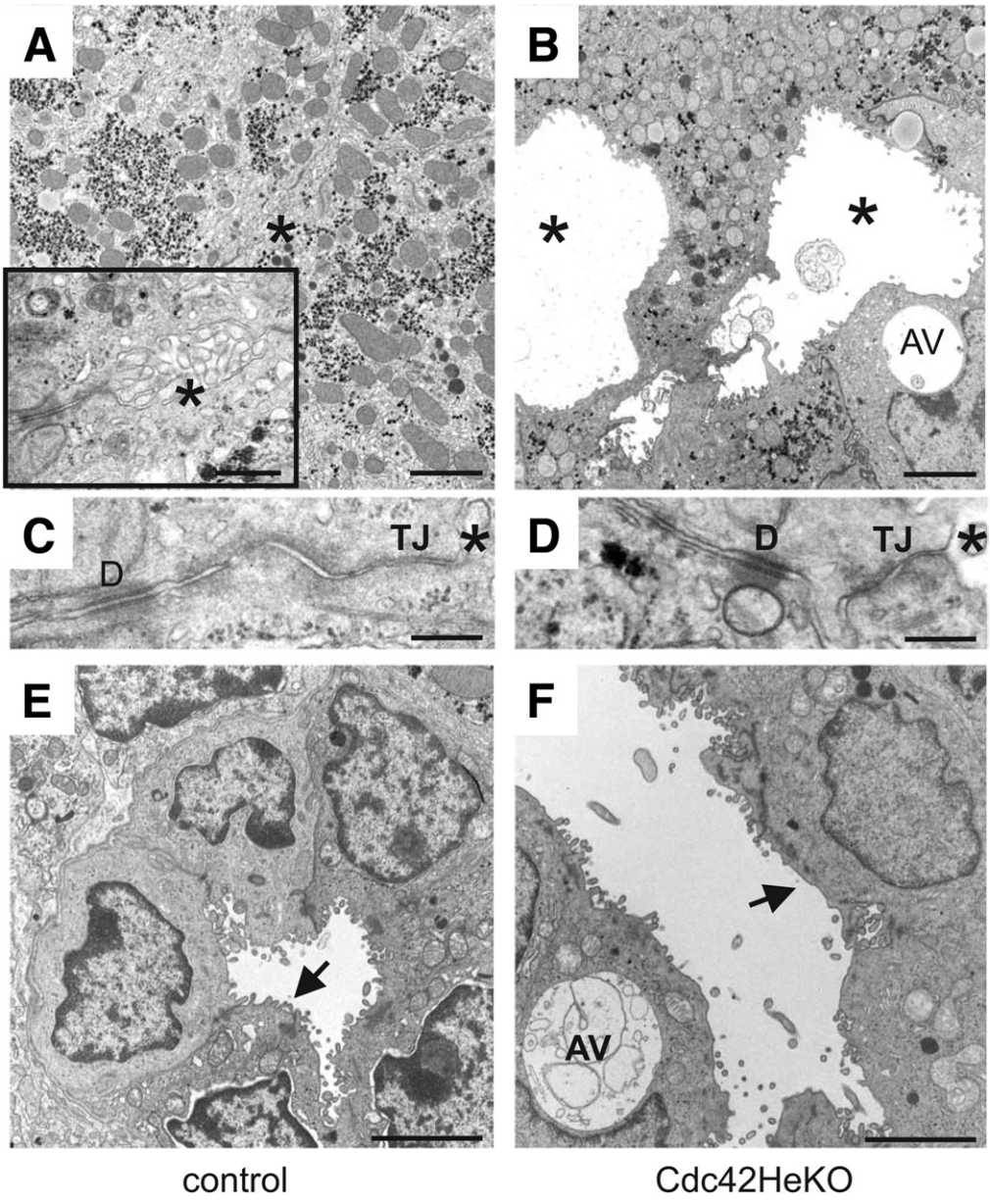

Figure 4. Ultrastructural analysis of livers: at lower magnification (*A*, *B*, *E*, and *F*; magnification bars, 2.5 μm), and higher magnification (inset in *A*; *C* and *D*; magnification bars, 250 nm). (*A* and *B*) Asterisks indicate bile canaliculi, confirming that hepatocytes remain polarized in the absence of Cdc42 although the canaliculi become much larger. Large cytoplasmic lumina, identified as anoxic vacuoles (AV), were observed in Cdc42HeKO hepatocytes (*C*–*F*). Desmosomes (D) and tight junctions (TJ) were identified in both (*C*) control and (*D*) Cdc42HeKO livers. (*E* and *F*) A bile duct from a control mouse shows regular architecture and small lumen. In contrast, a bile duct from a Cdc42HeKO mouse shows a widened lumen, cholangiocytes with AV, and fewer apical microvilli (arrow).

were still present. The amount of cytoplasmic glycogen was reduced and clustered in some hepatocytes. Remarkably, large anoxic vacuoles were observed in mutant hepatocytes (Figure 4*B*). In line with the histologically observed dysplasia, occasional hepatocytes presented dysplastic features, such as large irregular nuclei with vesicular inclusions and prominent nucleoli. Swollen mitochondria and an aberrant rough endoplasmic reticulum also were obvious in mutant hepatocytes.

Ultrastructurally, intrahepatic bile ducts in control mice were lined with a single layer of differentiated cuboidal epithelial cells with well-formed microvilli and cell junctions (Figure 4*E*). Compared with normal bile ducts, Cdc42-deficient ducts were dilated, and their cells showed fewer and irregular apical microvilli besides cytoplasmic anoxic vacuoles (Figure 4*F*).

Disturbance of Cell Junctions in Cdc42 Mutant Hepatocytes

To determine whether aberrant widening of the canaliculi could be caused by defects in cell–cell contacts, we examined the distribution of cell junctions. E-cadherin had zonal expression patterns in normal liver. Hepatocytes in the peripheral area of the lobules showed strong E-cadherin staining, as reported.[14] In Cdc42HeKO mice, E-cadherin was present at cell contacts of all hepatocytes and in bile ducts, which were highly abundant in these mice (Figure 5*A* and *B*). Further analysis revealed that all hepatocytes of both control and Cdc42HeKO

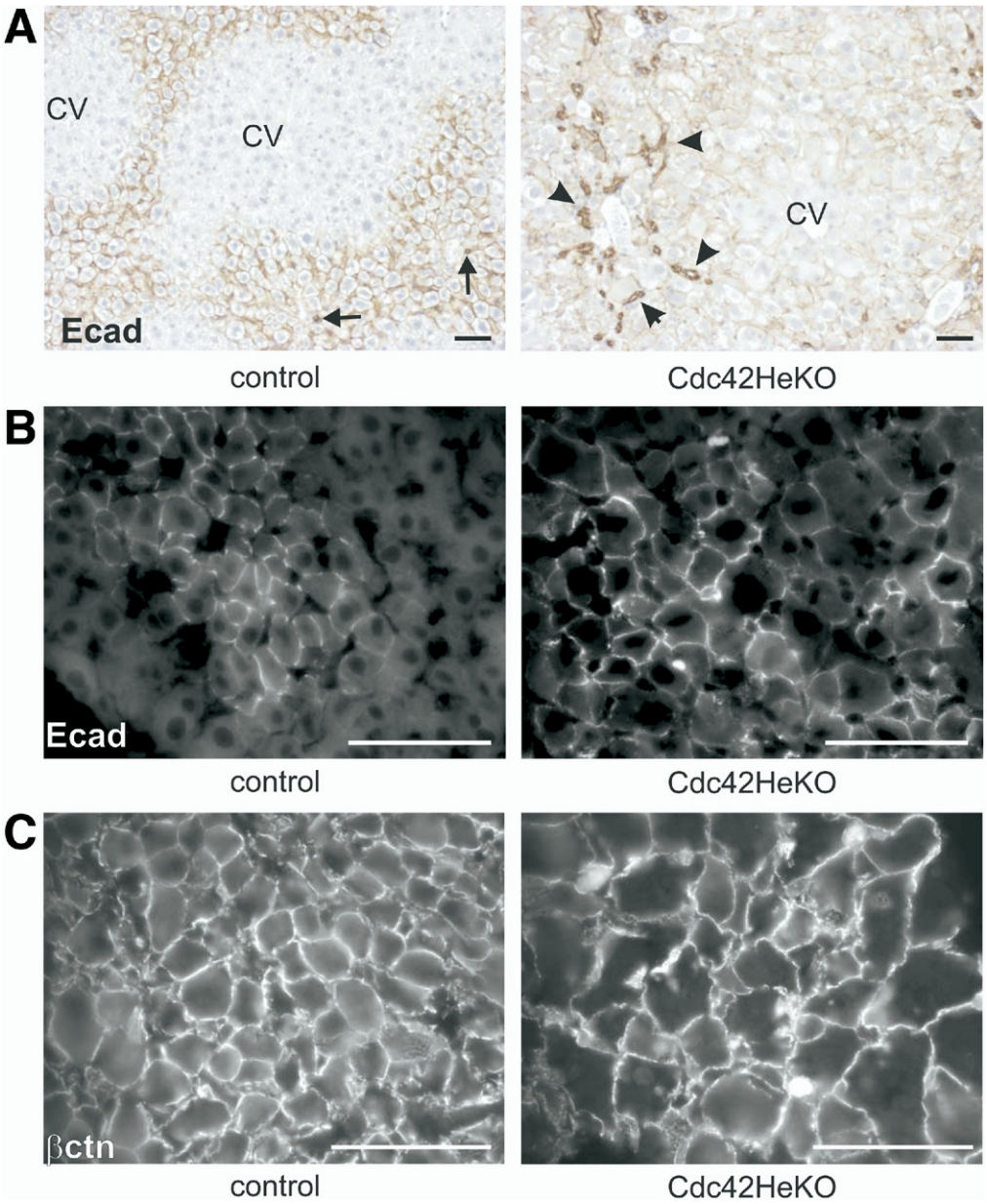

Figure 5. Adherens junctions are present in Cdc42HeKO livers. (*A*) In livers of control adult mice, hepatocytes in the peripheral area of the lobules were immunolabeled for E-cadherin. Arrows show bile ducts. CV, central vein. In contrast to normal livers, Cdc42-negative livers show E-cadherin staining in the center of the lobule. Arrowheads show ductular reaction, with bile duct cells expressing E-cadherin strongly. (*B*) Confocal immunofluorescent staining of E-cadherin in livers of 2-month-old mice. (*C*) Confocal immunofluorescent staining of β-catenin in livers of 9-month-old mice. Magnification bars, 100 μm.

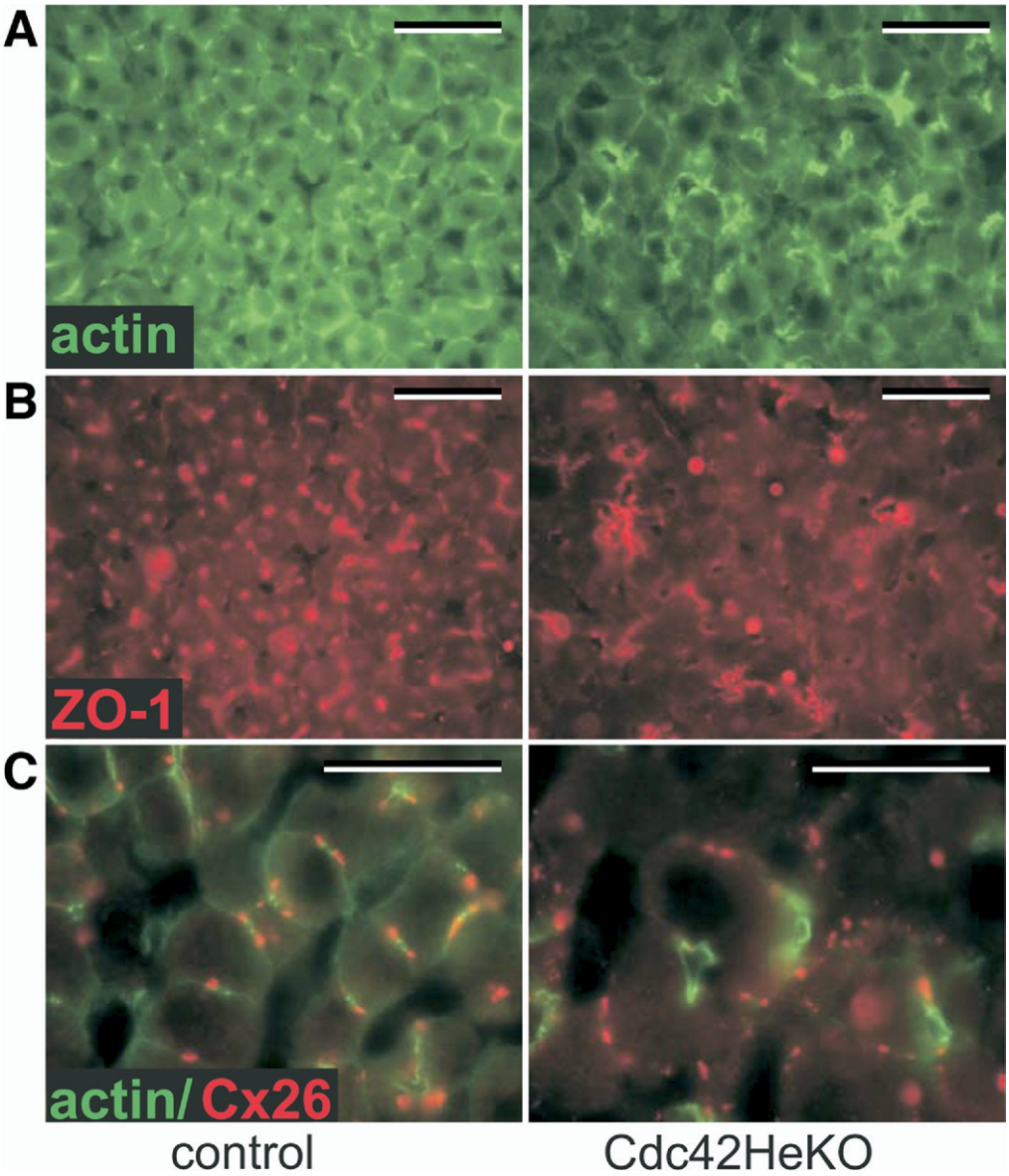

Figure 6. Alterations in cell junctions in Cdc42-deficient hepatocytes. Confocal double-immunofluorescent staining of (*A*) actin and (*B*) Z0-1 in livers of 2-month-old control and Cdc42HeKO mice. (*C*) Confocal double immunostaining of Cx26 (red) and F-actin (green) in control and Cdc42HeKO livers. Magnification bars, 50 μm.

mutant mice expressed N-cadherin homogeneously (supplementary Figure 5; see supplementary material online at www.gastrojournal.org). In total liver lysates more E-cadherin protein was detected in Cdc42HeKO livers (supplementary Figure 5*E*; see supplementary material online at www.gastrojournal.org). In both control and mutant livers, α-catenin, β-catenin, and p120ctn all were present in adherens junctions (shown for β-catenin in Figure 5*C*).

We analyzed other cell junctions in the liver by comparing immunostainings of liver sections from adult control and Cdc42HeKO mice. F-actin (Figure 6*A*) was present at the plasma membrane and enriched at the tight junctions, where it colocalized with zona occludens (Z0)-1 (Figure 6*B*), as well as with occludin and claudin-1 (data not shown). There was no difference between Cdc42-deficient hepatocytes and control hepatocytes in the expression level or colocalization of these tight junctional components. Staining patterns and morphometric analysis of phalloidin-stained tissue sections revealed that bile canaliculi in adult Cdc42-deficient livers were dilated (mean diameter, 9.41 $\pm$ 1.19 μm; 4 livers) compared with adult wild-type controls (mean diameter, 3.31 $\pm$ 0.66 μm; 4 livers). ZO-1, claudin-1, occludin, and actin proteins colocalized around the dilated bile canaliculi of Cdc42-negative hepatocytes.

Gap junctional proteins Cx32 and Cx26 were detected near the apical membrane of wild-type hepatocytes, as exemplified for Cx26 in Figure 6*C*. Cdc42-deficient hepatocytes still expressed both connexins at the plasma membrane, but not in the neighborhood of tight junctions.

Abnormal Bile Ducts in Cdc42 Mutant Livers

As described previously, bile ducts of Cdc42 mutant mice had an abnormal ultrastructure (Figure 4*F*).

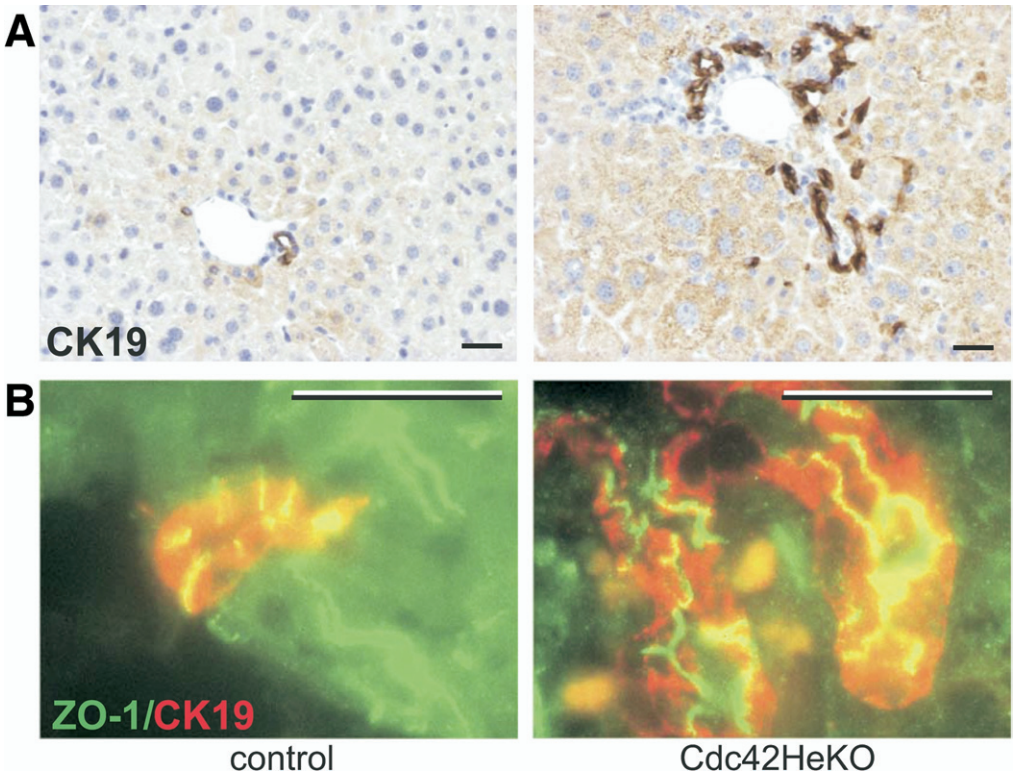

Figure 7. Bile ducts were more numerous in Cdc42HeKO mice than in their normal counterparts. (*A*) CK19 staining of livers from adult control and Cdc42HeKO mice. (*B*) Tight junctions are present in bile ducts from Cdc42HeKO livers, as revealed by double immunofluorescence of the tight junctional protein ZO-1 and of CK19 in control and Cdc42HeKO mice. Magnification bars, 50 μm.

Dilation of bile ducts in those mice was also evident by light microscopic examination of sections stained for CK19 (Figure 7*A*). Double immunofluorescent staining of CK19 and the tight junction protein ZO-1 was performed on age-matched Cdc42HeKO and control livers. Tight junctions were not altered severely in Cdc42HeKO livers (Figure 7*B*), as also shown by ultrastructural analysis. Increased proliferation of cholangiocytes in Cdc42HeKO livers was revealed by BrdU incorporation (data not shown).

The similar abnormalities observed in hepatocytes and cholangiocytes of intrahepatic bile ducts strongly indicate that Cdc42 was also deleted in bile duct cells. This may appear unlikely because deletion of Cdc42 is linked to the expression of albumin. However, intrahepatic bile ducts develop from albumin-expressing hepatoblasts that surround the portal tract. This also explains why the livers of the progeny of a cross between AlbCre mice and a Rosa26 reporter mouse contained both hepatocytes and cholangiocytes that were positive for β-galactosidase (supplementary Figure 2*B* and *C*; see supplementary material online at www.gastrojournal.org). By using an analogous AlbCre mouse line, Xu et al[15] recently made similar observations.

The CK19 stainings (Figure 7) also highlighted the occurrence of varying degrees of ductular reactions. Reactive ductules represent a reaction to damage to hepatocytes and/or bile duct cells.[16] In the current model, considerable damage indeed occurred in both the hepatocytic and biliary components.

Apical Par-Cdc42-aPKC Proteins Are Present in Cdc42 Mutant Hepatocytes

Par-3, Par-6, and one of the aPKCs, PKCζ, were localized immunohistochemically in the hepatocytes around the bile canaliculi in control mice and around dilated bile canaliculi of all sizes in Cdc42HeKO mice (exemplified for PKCζ in supplementary Figure 6; see supplementary material online at www.gastrojournal.org). These data indicate that localization of Par-3, Par-6, and PKCζ at the tight junctions is not dependent on Cdc42.

Discussion

We report here that Cdc42 deletion in the liver leads to HCC. The different stages of hepatocarcinogenesis were observed in the livers of Cdc42HeKO mice: oncocytic foci, small-cell dysplasia, and large-cell dysplasia. Damaged hepatocytes were visible at all the stages we analyzed. We showed that both the large dysplastic nodules and HCCs consist of Cdc42-negative hepatocytes. Hence, absence of Cdc42 confers a growth advantage. In our Cdc42HeKO mouse, different observed abnormalities might act as a tumor-promoting event, whereas absence of Cdc42 is the initiating agent. Cdc42HeKO livers showed changes in parenchymal canaliculi, and intrahepatic bile ducts were affected. Defects in both cell types decrease bile transport and lead to high levels of conjugated bilirubin.

Another prominent feature in Cdc42HeKO livers is the presence of anoxic vacuoles (Figure 4). We assume that these vacuoles are formed by invagination of the peripheral cell membrane or by de novo formation of plasma membranes, which has been reported for some cases of aspecific hepatocyte injury. Similar vacuoles were found in anoxic-resuscitated liver allografts,[17] in cells in tissue culture injured by ischemia or adenosine triphosphate depletion, in hepatocytes from mice with bile duct ligation, and in livers of mice treated with ethinyl estradiol.[18]

One defect that might cause the observed phenotypes is the prominent dilatation of bile canaliculi formed by Cdc42-deficient hepatocytes, possibly owing to the abnormal organization of the cytoskeleton near the apical membranes. We observed thickening of the pericanalicular ectoplasm, which is rich in actin filaments, and a prominent sheath of intermediate filaments around the ectoplasmic rim. The pericanalicular web plays an important role in peristalsis, transport of vesicles, and topography of transmembrane proteins. It is believed that bile transport in the canalicular system of the rodent liver is driven by the synchronous contraction of cytoskeletal elements of hepatocytes. Intercellular communication via gap junctional channels likely functions in synchronizing the contraction of neighboring hepatocytes. We observed that both Cx26 and Cx32 were expressed at an abnormal distance from the tight junctions in Cdc42HeKO hepatocytes.

The tight junction barrier may be affected in Cdc42HeKO hepatocytes, which would disrupt the blood-bile barrier and lead to leakage of bile acids, cell damage, and proliferation of hepatocytes and cholangiocytes. As recently reviewed, bile acids cause DNA damage and act as tumor promoters, in line with mutagenic and carcinogenic potential.[19] Alternatively, direct signaling by tight junctional proteins may regulate epithelial cell proliferation. We know very little about how polarity complexes signal and function in Cdc42-deficient hepatocytes and in normal hepatocytes. Our present analysis of tight junctional components did not reveal a major change in the composition of these junctions, although it is clear that the ultrastructure and size of the apical domains are affected strongly.

Although Cdc42 is a key activator of the Par complex in yeast,[20] its role in Par polarity signaling in vertebrate epithelial cells is less clear. Cdc42 activity in Madin-Darby canine kidney (MDCK) cells is dispensable for apical–basal cell polarization[21]; however, there is limited evidence for the involvement of Cdc42 in tight junction biogenesis. Two recent independent studies showed that Tiam1, a Rac activator directly associated with the Par polarity complex, controls tight junction assembly in MDCK and primary keratinocytes.[21,22] This may also occur in hepatocytes, including those of Cdc42HeKO livers, which would explain the minor Par polarity defects.

Several studies have shown that cadherin-mediated signaling is involved in the contact-dependent inhibition of growth. Contact-induced proliferation arrest mediated by $p27^{Kip1}$ was reported to be initiated by the activation of cadherin signaling.[23,24] Reduced E-cadherin expression, such as we observed in hepatocytes of the peripheral area of Cdc42HeKO liver lobules, thus may contribute to their increased proliferation rate.

The earlier-described alterations in cell junctions are rather subtle compared with the effects of Cdc42 deletion in the epidermis,[6] or neuroepithelia,[7,8] in which Cdc42 deficiency leads to gradual loss of the Par complex and/or adherens junctions. Even in Cdc42-deficient livers from aged mice, cadherin, catenins, and the Par-complex remained at the plasma membrane. These results underline the importance of studying the role of Cdc42 in diverse tissues because this Rho-GTPase exerts rather distinct functions in different cell types.

Characteristic genomic alterations in HCC can be used to divide these tumors into 2 broad categories. The major features of the first category are chromosomal stability with activation of the Wnt/Wingless pathway by disruption of β-catenin function, whereas the second category is characterized by chromosomal instability.[25,26] Because we detected neither cytoplasmic nor nuclear translocation of β-catenin in Cdc42-deficient hepatocytes, nor any evidence for β-catenin mutations, Cdc42HeKO livers may belong to the second category. HCC grows slowly in Cdc42 deficient livers, possibly owing to the lack of Wnt/β-catenin activation.

In the earlier-described hypotheses, cell junctional abnormalities in Cdc42-deficient liver cells are considered the primary defect, and hepatomegaly an indirect consequence. Nevertheless, induction of cell proliferation as a direct effect of the Cdc42 deficiency cannot be excluded. Multiple studies have shown a role for Cdc42 in promoting cell-cycle progression.[27,28] According to another report, Cdc42 is not sufficient by itself, but nevertheless promotes proliferation and G1 progression.[29] Hepatocytes and cholangiocytes devoid of Cdc42 displayed an accelerated rather than a diminished proliferation rate. In this regard it is also noteworthy that Cdc42 transcripts were induced strongly in a rat model of partial hepatectomy and liver regeneration.[30] This finding and our data on Cdc42 mutant mice support a regulatory role for Cdc42 as a cell-cycle gene in hepatocytes.

HCC in Cdc42HeKO mice develops with high penetrance and follows the histopathologic progression of HCC described in chronic liver disease, including development of metastases in the lungs. We started by analyzing Cdc42 expression and activity in human HCC. A preliminary analysis of published microarray data (see supplementary Figure 7*A*; see supplementary material online at www.gastrojournal.org) indicated that analysis of Cdc42 mRNA is probably not the most appropriate approach. Analysis of Cdc42 activity may be more rele-

vant. To determine whether Cdc42 activation is altered in human HCC, we analyzed array data of Cdc42-activating guanine nucleotide-exchange factors and of Cdc42-inactivating GTPase-activating proteins (GAPs) (supplementary Figure 7*B–C*; see supplementary material online at www.gastrojournal.org). An even more relevant experiment would be to analyze the activity of Cdc42 by pull-down assays using the GST-PAK1 effector domain.

HCC is a heterogeneous disease in terms of its etiology and biologic and clinical behavior. Very little is known about how many genes participate at the molecular level in tumor development, progression, and aggressiveness. Development of HCC is observed in several mouse models, such as hepatitis C virus (HCV)-transgenic mice.[31] Generation of certain deficiencies in mouse liver, such as inactivation of the tumor-suppressor gene adenomatous polyposis coli,[32] can lead to hyperplasia or even HCC. In other genetic mouse models, additional triggers such as treatment with a hepatocarcinogen may be needed to generate HCC. For example, although the retinoblastoma (RB) tumor-suppressor pathway is inactivated frequently in HCC, RB-deficient mouse livers do not develop tumors, indicating that RB loss by itself is not sufficient for liver tumorigenesis.[33] Other liver-specific gene deficiencies, such as the Cdc42 deletion in our model, were not expected to lead to development of HCC. One elegant model of HCC development is the c-myc/transforming growth factor-α double-transgenic mouse. Some of these mice start to develop HCC by the age of 4 months, and by 8 months all of them show the pathology.[34] These carcinomas metastasize, and mice die within 1 year. Development of HCC in Cdc42HeKO mice is slower than in c-myc/transforming growth factor-α double-transgenic mice, but it may be a useful model for human HCC, which develops mainly in older people.

Supplementary Data

Note: To access the supplementary material accompanying this article, visit the online version of *Gastroenterology* at www.gastrojournal.org, and at doi:10.1053/j.gastro.2008.01.002.

References

1. Vinken M, Papeleu P, Snykers S, et al. Involvement of cell junctions in hepatocyte culture functionality. Crit Rev Toxicol 2006; 36:299–318.
2. Temme A, Stumpel F, Sohl G, et al. Dilated bile canaliculi and attenuated decrease of nerve-dependent bile secretion in connexin32-deficient mouse liver. Pflugers Arch 2001;442: 961–966.
3. Margolis B, Borg JP. Apicobasal polarity complexes. J Cell Sci 2005;118:5157–5159.
4. Qiu RG, Abo A, Martin GS. A human homolog of the C-elegans polarity determinant Par-6 links Rac and Cdc42 to PKC zeta signaling and cell transformation. Curr Biol 2000;10:697–707.
5. Chen F, Ma L, Parrini MC, et al. Cdc42 is required for PIP2-induced actin polymerization and early development but not for cell viability. Curr Biol 2000;10:758–765.
6. Wu XW, Quondamatteo F, Brakebusch C. Cdc42 expression in keratinocytes is required for the maintenance of the basement membrane in skin. Matrix Biol 2006;25:466–474.
7. Cappello S, Attardo A, Wu XW, et al. The Rho-GTPase cdc42 regulates neural progenitor fate at the apical surface. Nat Neurosci 2006;9:1099–1107.
8. Chen L, Liao G, Yang L, et al. Cdc42 deficiency causes Sonic hedgehog-independent holoprosencephaly. Proc Natl Acad Sci U S A 2006;103:16520–16525.
9. Sahai E, Marshall CJ. Rho-GTPases and cancer. Nat Rev Cancer 2002;2:133–142.
10. Valentijn LJ, Koppen A, van Asperen R, et al. Inhibition of a new differentiation pathway in neuroblastoma by copy number defects of N-myc, Cdc42, and nm23 genes. Cancer Res 2005;65:3136–3145.
11. Limpaiboon T, Tapdara S, Jearanaikoon P, et al. Prognostic significance of microsatellite alterations at 1p36 in cholangiocarcinoma. World J Gastroenterol 2006;12:4377–4382.
12. Wu XW, Quondamatteo F, Lefever T, et al. Cdc42 controls progenitor cell differentiation and beta-catenin turnover in skin. Genes Dev 2006;20:571–585.
13. Postic C, Magnuson MA. DNA excision in liver by an albumin-Cre transgene occurs progressively with age. Genesis 2000;26: 149–150.
14. Fujimoto K, Nagafuchi A, Tsukita S, et al. Dynamics of connexins, E-cadherin and alpha-catenin on cell membranes during gap junction formation. J Cell Sci 1997;110:311–322.
15. Xu X, Kobayashi S, Qiao W, et al. Induction of intrahepatic cholangiocellular carcinoma by liver-specific disruption of Smad4 and Pten in mice. J Clin Invest 2006;116:1843–1852.
16. Libbrecht L, Roskams T. Hepatic progenitor cells in human liver diseases. Semin Cell Dev Biol 2002;13:389–396.
17. Jurado F, Bujan J, Mora NP, et al. A histopathological study of anoxic-resuscitated liver allografts. Histol Histopathol 1997;12: 123–133.
18. Torok NJ, Larusso EM, McNiven MA. Alterations in vesicle transport and cell polarity in rat hepatocytes subjected to mechanical or chemical cholestasis. Gastroenterology 2001;121:1176–1184.
19. Bernstein H, Bernstein C, Payne CM, et al. Bile acids as carcinogens in human gastrointestinal cancers. Mutat Res 2005;589: 47–65.
20. Etienne-Manneville S. Cdc42—the centre of polarity. J Cell Sci 2004;117:1291–1300.
21. Mertens AEE, Rygiel TP, Olivo C, et al. The Rac activator Tiam1 controls tight junction biogenesis in keratinocytes through binding to and activation of the Par polarity complex. J Cell Biol 2005;170:1029–1037.
22. Chen XY, Macara IG. Par-3 controls tight junction assembly through the Rac exchange factor Tiam1. Nat Cell Biol 2005;7: 262–272.
23. Levenberg S, Yarden A, Kam Z, et al. p27 is involved in N-cadherin-mediated contact inhibition of cell growth and S-phase entry. Oncogene 1999;18:869–876.
24. St Croix B, Sheehan C, Rak JW, et al. E-cadherin-dependent growth suppression is mediated by the cyclin-dependent kinase inhibitor p27(KIP1). J Cell Biol 1998;142:557–571.
25. Laurent-Puig P, Zucman-Rossi J. Genetics of hepatocellular tumors. Oncogene 2006;25:3778–3786.
26. Legoix P, Bluteau O, Bayer J, et al. Beta-catenin mutations in hepatocellular carcinoma correlate with a low rate of loss of heterozygosity. Oncogene 1999;18:4044–4046.
27. Lamarche N, Tapon N, Stowers L, et al. Rac and Cdc42 induce actin polymerization and G1 cell cycle progression independently of p65PAK and the JNK/SAPK MAP kinase cascade. Cell 1996; 87:519–529.

28. Lin R, Bagrodia S, Cerione R, et al. A novel Cdc42Hs mutant induces cellular transformation. Curr Biol 1997;7:794–797.
29. Qiu RG, Abo A, McCormick F, et al. Cdc42 regulates anchorage-independent growth and is necessary for Ras transformation. Mol Cell Biol 1997;17:3449–3458.
30. Cimica V, Batusic D, Chen Y, et al. Transcriptome analysis of rat liver regeneration in a model of oval hepatic stem cells. Genomics 2005;86:352–364.
31. Ernst E, Schonig K, Bugert JJ, et al. Generation of inducible hepatitis C virus transgenic mouse lines. J Med Virol 2007;79:1103–1112.
32. Colnot S, Decaens T, Niwa-Kawakita M, et al. Liver-targeted disruption of Apc in mice activates beta-catenin signaling and leads to hepatocellular carcinomas. Proc Natl Acad Sci U S A 2004;101:17216–17221.
33. Mayhew CN, Bosco EE, Fox SR, et al. Liver-specific pRB loss results in ectopic cell cycle entry and aberrant ploidy. Cancer Res 2005;65:4568–4577.
34. Santoni-Rugiu E, Nagy P, Jensen MR, et al. Evolution of neoplastic development in the liver of transgenic mice co-expressing c-myc and transforming growth factor-alpha. Am J Pathol 1996;149:407–428.

Received December 2, 2006. Accepted December 6, 2007.

Address requests for reprints to: Frans van Roy, PhD, Department for Molecular Biomedical Research, VIB & Ghent University, Technologiepark 927, B-9052 Ghent, Belgium. e-mail: F.Vanroy@dmbr.UGent.be; fax: (32) 9-3313-500.

This research was supported by the National Fund for Scientific Research-Flanders, the Max Planck Society, and the German Research Council. The German Mouse Clinic is funded by grant 01GR0430 from Bundesministerium fur Bildung und Forschung, Nationales Genomforschungsnetz, Germany.

The authors thank Dr. Reinhard Fässler for his generous support, Dr. Pieter De Bleser for the statistical analysis, and Dr. Amin Bredan for critical reading of the manuscript.

Present address of X.W.: Cutaneous Biology Research Center, Massachusetts General Hospital, Harvard Medical School, Charlestown, Massachusetts; present address of F.Q.: Department of Anatomy, National University of Ireland, Galway, Ireland; and present address of C.B.: University of Copenhagen, Institute of Molecular Pathology, Copenhagen, Denmark.